D^0–$\overline{D}^0$ MIXING IN $D^0 \to K\pi^*$

Michael D. Sokoloff

for the BaBar Collaboration

University of Cincinnati, Cincinnati, OH 45208 USA

(Received January 8, 2008)

Recently, the BaBar collaboration presented evidence for $D^0 - \overline{D}^0$ mixing in $D^0 \to K^+\pi^-$ decays from $384\,\mathrm{fb}^{-1}$ of e^+e^- colliding-beam data recorded near $\sqrt{s} = 10.6\,\mathrm{GeV}$. The reported mixing parameters are $x'^2 = [-0.22 \pm 0.30(\mathrm{stat.}) \pm 0.21(\mathrm{syst.})] \times 10^{-3}$ and $y' = [9.7 \pm 4.4(\mathrm{stat.}) \pm 3.1(\mathrm{syst.})] \times 10^{-3}$ with correlation coefficient -0.94. This excludes the no-mixing hypothesis at the $3.9\,\sigma$ level. Earlier results from the BELLE collaboration excluded the no-mixing hypothesis at the $2\,\sigma$ level and are consistent with BaBar's. Combining these results, the no-mixing hypothesis is excluded at the $4\,\sigma$ level. No evidence for CP violation is observed.

PACS numbers: 13.25.Ft, 12.15.Ff, 11.30.Er

1. Introduction

The D^0 and $\overline{D}^0$ mesons are flavor eigenstates which contain c and $\overline{c}$ quarks, respectively. These mesons decay, instead, as mass and lifetime eigenstates. This allows initial flavor eigenstates, produced in strong interactions, to evolve into mixtures of D^0 and $\overline{D}^0$. In the Standard Model (SM), such oscillations can proceed through short-distance amplitudes and the expected mixing rate mediated by SM box [1] and di-penguin [2] amplitudes is $\mathcal{O}(10^{-8}$–$10^{-10})$, well below the current experimental sensitivity of $\mathcal{O}(10^{-4}$–$10^{-3})$ [3]. Long-distance enhancements to the SM mixing rate involve non-perturbative effects. Predictions range over many orders of magnitude [4–8] approximately bounded by the box diagram rate and current experimental sensitivity. New physics (NP) predictions span the same large range [8]. Thus, observation of mixing at the current level of sensitivity is not a clear indication of new physics, but it invites better calculations of SM long-distance effects and more precise measurements.

* Presented at the Symposium "Physics in Collision", Annecy, France, June 26–29, 2007.

2. Mixing formalism and model predictions

The neutral D mesons studied in these analyses are produced in charged D^* decays, and are flavor eigenstates at the time of D^* decay. The D^0 and $\overline{D}^0$ mesons, in turn, evolve and decay as eigenstates of the equation

$$\frac{\partial}{\partial t}\begin{pmatrix} D^0(t) \\ \overline{D}^0(t) \end{pmatrix} = \boldsymbol{H}\begin{pmatrix} D^0(t) \\ \overline{D}^0(t) \end{pmatrix}, \qquad \boldsymbol{H} = \boldsymbol{M} - \frac{i}{2}\boldsymbol{\varGamma}, \tag{1}$$

with masses and widths M_1, $\varGamma_1$ and M_2, $\varGamma_2$. The oscillations of D^0 into $\overline{D}^0$, and *vice versa*, commonly referred to as mixing, depend on the mass and decay rate differences $\Delta M = M_1 - M_2$ and $\Delta\varGamma = \varGamma_1 - \varGamma_2$. When characterizing mixing, we often use the more compact, dimensionless variables

$$x = \frac{\Delta M}{\varGamma}, \qquad y = \frac{\Delta\varGamma}{2\varGamma}, \tag{2}$$

where $\varGamma$ is the average of $\varGamma_1$ and $\varGamma_2$.

Following Ref. [9], the expansion of the off-diagonal terms in the Hamiltonian to second order in perturbation theory can be written

$$\begin{aligned}\left(M - \frac{i}{2}\varGamma\right)_{12} = {} & \frac{1}{2m_D}\langle D^0|\mathcal{H}_w^{\Delta C=2}|\overline{D}^0\rangle \\ & + \frac{1}{2m_D}\sum_n \frac{\langle D^0|\mathcal{H}_w^{\Delta C=1}|n\rangle\,\langle n|\mathcal{H}_w^{\Delta C=1}|\overline{D}^0\rangle}{m_D - E_n + i\epsilon}\,.\end{aligned} \tag{3}$$

The first term represents the "short-distance", $\Delta C = 2$ contributions. It contributes only to ΔM and is expected to be very small in the Standard Model. The second term represents the "long-distance" contributions, and it contributes to both ΔM and $\Delta\varGamma$. As discussed in Ref. [10], if one neglects the contributions of b quarks, mixing vanishes in the flavor SU(3) limit, and it only arises at second order in SU(3) breaking:

$$x,\, y \sim \sin^2\theta_{\rm C} \times [\mathrm{SU(3)\ breaking}]^2\,, \tag{4}$$

where $\theta_{\rm C}$ is the Cabibbo angle. In 1985 Wolfenstein noted that SU(3) is badly broken in D^0 decays to $\pi^-\pi^+$ and K^-K^+ and suggested $x, y \sim \mathcal{O}(1\%)$ was possible in the SM [4]. A somewhat more detailed calculation of dispersive effects [5] suggested that x would be enhanced relative to the box diagram rate, but it would be $\lesssim 10^{-3}$. Subsequently, inclusive calculations [6,7] of ΔM and $\Delta\varGamma$ based on the operator product expansion, which rely on local quark–hadron duality, predicted $x, y \lesssim 10^{-3}$. More recently, the size of SU(3) violation in exclusive contributions to y due to phase space differences have been explored [10]. The authors assume there are no cancellations with other sources of SU(3) breaking that would reduce their result by an order of magnitude; they explain that this is equivalent to assuming that the D meson is not heavy enough that duality can be expected to enforce such cancellations. With these caveats, they find $y \sim \mathcal{O}(1\%)$. A related calculation of ΔM from a dispersion relation [9] suggests that if y is in the ballpark of $+1\%$ then one should expect $|x|$ between 10^{-3} and 10^{-2}, with x and y of opposite sign. The authors caution that this estimate has a large uncertainty, and that they trust it only at the order of magnitude level.

Some SM estimates for y and x do not exclude values near 1%. Thus, observations of mixing with parameters in this range do not necessarily indicate new physics. However, various NP scenarios produce contributions to x and y which are of potential interest. A recent paper [11], which also summarizes SM calculations very well, reviews predictions from a variety of NP models. These include models with extra fermions, extra gauge bosons, extra scalars, extra space dimensions, or extra symmetries. Some models require multiple new features to avoid bounds from precision electroweak measurements. Perhaps surprisingly, the authors identify almost 20 types of models where current measurements constrain the parameters. This sensitivity to the types of NP which will produce dramatic signals at the LHC highlights the complementarity of charm mixing measurements for understanding NP origins when direct signals are observed more directly.

Searching for $D^0 - \overline{D}^0$ mixing using the $D^0 \to K\pi$ final states has a long history. The Cabibbo-favored (CF) decay $D^0 \to K^-\pi^+$ enjoys a large branching fraction and relatively low combinatorial backgrounds. Historically, CF decays are also referred to as right-sign (RS) decays while the decay $D^0 \to K^+\pi^-$ is referred to as a wrong-sign (WS) decay. The latter can be produced via a doubly Cabibbo-suppressed (DCS) amplitude or via mixing followed by a CF decay. The relative momenta of the quarks forming the final state hadrons in the DCS and mixed amplitudes differ, producing a strong phase, $\delta_{K\pi}$, between the two amplitudes which becomes important when they interfere. DCS decays have small rates, R_{D}, typically of order $\tan^4\theta_{\mathrm{C}} \approx 0.3\%$ relative to their CF partners. Early mixing searches, which were not sensitive to WS signals at the DCS rate, looked for WS signals as a signature of mixing. As the sizes of D^0 samples have increased, searches have looked at the time-dependence of WS signals for evidence of mixing as well as DCS amplitudes. For $D^0 \to K\pi$, and in the limits of CP conservation and small mixing ($|x|, |y| \ll 1$), we approximate the WS time-dependence:

$$\frac{T_{\mathrm{WS}}(t)}{e^{-\Gamma t}} \propto R_{\mathrm{D}} + \sqrt{R_{\mathrm{D}}}y'\,\Gamma t + \frac{x'^2 + y'^2}{4}\,(\Gamma t)^2\,, \tag{5}$$

where $x' = x\cos\delta_{K\pi} + y\sin\delta_{K\pi}$, $y' = -x\sin\delta_{K\pi} + y\cos\delta_{K\pi}$.

3. BaBar's recent $K\pi$ analysis

The BaBar Collaboration recently reported an analysis of 384 fb^{-1} e^+e^- colliding-beam data recorded near $\sqrt{s} = 10.6$ GeV at the PEP-II asymmetric-energy storage rings. Here, I repeat a few of the most important elements of the analysis [12]. The flavors of neutral D mesons at production are identified by restricting the sample to decay products of charged D^* decay, for example, $D^{*+} \to \pi_s{}^+ D^0$ where the $\pi_s{}^+$ is referred to as the "slow pion". In RS decays the $\pi_s{}^+$ and kaon have opposite charges, while in WS decays the charges are the same. Candidate $D \to K\pi$ pairs are selected by pairing oppositely-charged tracks with $K^\mp\pi^\pm$ invariant mass $m_{K\pi}$ between 1.81 and 1.92 GeV/c^2. Each pair is identified as $K^\mp\pi^\pm$ using a likelihood-based particle identification algorithm. The identification efficiency for kaons (pions) is about 85% (95%); the misidentification rate of kaons (pions) as pions (kaons) is about 2% (6%).

To obtain the proper decay time t and its error σ_t for each D^0 candidate, the $K^\mp$ and $\pi^\pm$ tracks are refit, constraining them to originate from a common vertex. The D^0 and $\pi_s{}^+$ are required to originate from a common vertex, constrained by the position and size of the e^+e^- interaction region. The $\pi_s{}^+$ must have momentum in the laboratory frame greater than 0.1 GeV/c and in the e^+e^- center-of-mass (CM) frame below 0.45 GeV/c. The χ^2 probability of the vertex-constrained combined fit $P(\chi^2)$ must be at least 0.1%, and the $m_{K\pi\pi} - m_{K\pi}$ mass difference Δm must lie in the range $0.14 < \Delta m < 0.16$ GeV/c^2. To remove D^0 candidates from B-meson decays and to reduce combinatorial backgrounds, each D^0 is required to have a momentum in the CM frame greater than 2.5 GeV/c. The analysis also requires $-2 < t < 4$ ps and $\sigma_t < 0.5$ ps (the most probable value of σ_t for signal events is 0.16 ps). For D^{*+} candidates sharing one or more tracks with other D^{*+} candidates, only the candidate with the highest $P(\chi^2)$is retained. After applying all criteria, approximately 1 229 000 RS and 64 000 WS D^0 and $\overline{D}^0$ candidates are selected. Projections of the WS data, and of the fit discussed below, are shown in Fig. 1. To avoid potential bias, the data selection criteria and the procedures for fitting and extracting the statistical limits were finalized without examining the mixing results.

The mixing parameters are determined in an unbinned, extended maximum likelihood fit to the RS and WS data samples over the four observables $m_{K\pi}$, Δm, t, and σ_t. The fit is performed in several stages. First, RS and WS signal and background shape parameters are determined from a fit to $m_{K\pi}$ and Δm, and are not varied in subsequent fits. Next, the D^0 proper-time resolution function and lifetime are determined in a fit to the RS data using $m_{K\pi}$ and Δm to separate the signal and background components.

Finally, the WS data sample is fit three times: once assuming CP conservation and no mixing, then assuming CP conservation but allowing mixing, and finally allowing both mixing and CP violation.

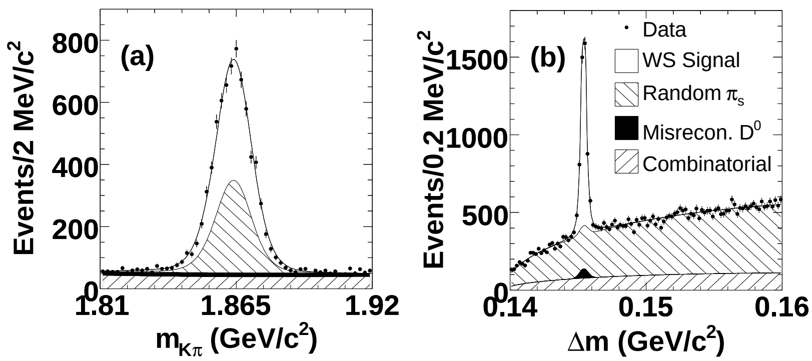

Fig. 1. (a) $m_{K\pi}$ for WS candidates with $0.1445 < \Delta m < 0.1465\,\mathrm{GeV}/c^2$, and (b) Δm for WS candidates with $1.843 < m_{K\pi} < 1.883\,\mathrm{GeV}/c^2$. The fitted PDFs are overlaid. The shaded regions represent the different background components.

The RS and WS $\{m_{K\pi}, \Delta m\}$ distributions are described by four components: signal, random ${\pi_s}^+$, misreconstructed D^0 and combinatorial background. Signal peaks characteristically in both $m_{K\pi}$ and Δm. The random ${\pi_s}^+$ component models reconstructed D^0 decays combined with a random slow pion and has the same shape in $m_{K\pi}$ as signal events, but does not peak in Δm. Misreconstructed D^0 events have one or more of the D^0 decay products either not reconstructed or reconstructed with the wrong particle hypothesis. They peak in Δm, but not in $m_{K\pi}$. Combinatorial background events are those not described by the above components; they do not exhibit any peaking structure in $m_{K\pi}$ or Δm. The functional forms of the probability density functions (PDFs) for the signal and background components are chosen based on studies of Monte Carlo (MC) samples. However, all parameters are determined from two-dimensional likelihood fits to data over the full region $1.81 < m_{K\pi} < 1.92\,\mathrm{GeV}/c^2$ and $0.14 < \Delta m < 0.16\,\mathrm{GeV}/c^2$.

The RS and WS $(m_{K\pi}, \Delta m)$ data are fit simultaneously with shared shape parameters describing the signal and random ${\pi_s}^+$ components common to both samples. There are $1\,141\,500 \pm 1\,200$ RS signal events and $4\,030 \pm 90$ WS signal events. The dominant background component is the random ${\pi_s}^+$ background. Fig. 1 shows projections of the WS data and fit.

The RS proper decay-time distribution is fit over all events in the full $m_{K\pi}$ and Δm region. The PDFs for signal and background in $(m_{K\pi}, \Delta m)$ are used in the decay-time fit with all parameters fixed to their previously determined values. The measured decay-time distribution for RS signal is described by an exponential function convolved with a resolution function whose parameters are determined by the fit to the data. The resolution function is the sum of three Gaussians with widths proportional to the estimated event-by-event proper-time uncertainty σ_t. The random ${\pi_s}^+$ background is described by the same proper-time distribution as signal events, since the slow pion has little weight in the vertex fit. The proper-time distribution of the combinatorial background is described by a sum of two Gaussians, one of which has a power-law tail to account for a small long-lived component. The combinatorial background and real D^0 decays have different σ_t distributions, as determined from data using a background-subtraction technique [13] based on the fit to $m_{K\pi}$ and Δm.

The measured decay-time distribution for WS signal is modeled first (no-mixing) as the RS exponential convolved with its resolution function, and second (mixing allowed, no CP violation) as Eq. (5) convolved with the RS resolution function. The random ${\pi_s}^+$ and misreconstructed D^0 backgrounds are described by the RS signal decay-time distribution since they are real D^0 decays. The parameters from these fits are listed in Table I.

TABLE I

Results from the different fits. The first uncertainty listed is statistical and the second systematic.

Fit type	Parameter	Fit results ($/10^{-3}$)
No CP viol. or mixing	R_D	$3.53 \pm 0.08 \pm 0.04$
No CP violation	R_D	$3.03 \pm 0.16 \pm 0.10$
	x'^2	$-0.22 \pm 0.30 \pm 0.21$
	y'	$9.7 \pm 4.4 \pm 3.1$
CP violation allowed	R_D	$3.03 \pm 0.16 \pm 0.10$
	A_D	$-21 \pm 52 \pm 15$
	x'^{2+}	$-0.24 \pm 0.43 \pm 0.30$
	y'^+	$9.8 \pm 6.4 \pm 4.5$
	x'^{2-}	$-0.20 \pm 0.41 \pm 0.29$
	y'^-	$9.6 \pm 6.1 \pm 4.3$

An easy way to visualize the data, and compare them to the results of the fit, is to examine the RS/WS ratio as a function of time shown in Fig. 2. As a cross-check, independent $\{m_{K\pi}, \Delta m\}$ fits were performed, with no shared parameters, for WS and RS samples for intervals in proper time selected to have approximately equal numbers of RS candidates. This ratio is seen to increase with time. The slope is consistent with the measured mixing parameters and inconsistent with the no-mixing hypothesis: the χ^2 with respect to expectation for the no-mixing hypothesis (a constant WS rate) is 24.0 for 5 bins, while that for the mixing fit is 1.5.

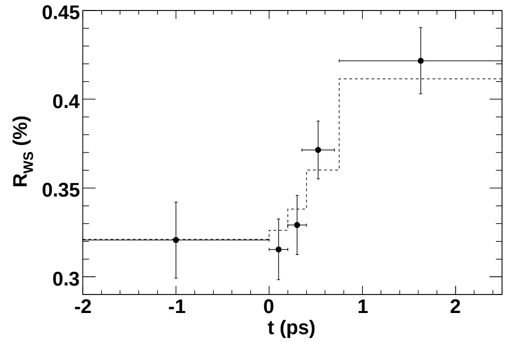

Fig. 2. The WS/RS ratio of branching fractions from independent $\{m_{K\pi}, \Delta m\}$ fits for slices in measured proper time (points). The dashed line shows the expected wrong-sign rate as determined from the mixing fit without CP violation.

The fit with mixing describes the data much better than does the fit with no mixing. The significance of the mixing signal is evaluated based on the change in negative log likelihood $(-2\Delta \ln \mathcal{L})$ with respect to the minimum. Fig. 3 shows confidence-level (CL) contours calculated from $-2\Delta \ln \mathcal{L}$ in two dimensions (x'^2, y') with systematic uncertainties included. The likelihood is maximum at the unphysical point $(x'^2 = -2.2 \times 10^{-4}, y' = 9.7 \times 10^{-3})$. The value of $-2\Delta \ln \mathcal{L}$ at the most likely point in the physically allowed region $(x'^2 = 0, y' = 6.4 \times 10^{-3})$ is 0.7 units. The value of $-2\Delta \ln \mathcal{L}$ for no-mixing

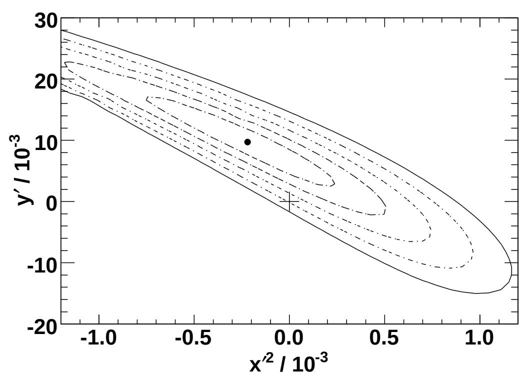

Fig. 3. The central value (point) and confidence-level contours for $1 - \mathrm{CL} = 0.317(1\sigma)$, 4.55×10^{-2} (2σ), $2.70 \times 10^{-3}(3\sigma)$, 6.33×10^{-5} (4σ) and $5.73 \times 10^{-7}(5\sigma)$, calculated from the change in the value of $-2 \ln \mathcal{L}$ compared with its value at the minimum. Systematic uncertainties are included. The no-mixing point is shown as a plus sign (+).

is 23.9 units. Including the systematic uncertainties [12], this corresponds to a significance equivalent to 3.9σ ($1 - \mathrm{CL} = 1 \times 10^{-4}$). The correlation coefficient between the x'^2 and y' parameters is -0.94.

To search for CP violation, the D^0 and $\overline{D}^0$ samples are fit separately for the parameters $\{R_{\mathrm{D}}^{\pm}, x'^{2\pm}, y'^{\pm}\}$ where the superscript $+$ $(-)$ denotes $D^0(\overline{D}^0)$ decays. The resulting values of $R_{\mathrm{D}} = \sqrt{{R_{\mathrm{D}}}^+ {R_{\mathrm{D}}}^-}$ and $A_{\mathrm{D}} = ({R_{\mathrm{D}}}^+ - {R_{\mathrm{D}}}^-)/({R_{\mathrm{D}}}^+ + {R_{\mathrm{D}}}^-)$ are listed in Table I. The best fit in each case is more than 3 σ from the no-mixing hypothesis, and there is no evidence of CP violation. All cross checks indicate that the high level of agreement between the separate D^0 and $\overline{D}^0$ fits is a coincidence.

4. Summary and conclusions

The results from the BaBar analysis [12] discussed above are consistent with the results of an earlier analysis of BELLE data [14] which reported central values $x'^2 = (0.18^{+0.21}_{-0.23}) \times 10^{-3}$, $y' = (0.6^{+4.0}_{-3.6}) \times 10^{-3}$ and a 3.9% confidence level for the no-mixing hypothesis (assuming no CP violation). Combining the BaBar and BELLE results in three dimensions, the Heavy Flavor Averaging Group [15] finds that the no-mixing hypothesis is excluded with greater than $4\,\sigma$ significance with central values $R_{\mathrm{D}} = (3.31 \pm 0.13)$ $\times 10^{-3}$, $x'^2 = (-0.01 \pm 0.20) \times 10^{-3}$, and $y' = (5.1 \pm 3.2) \times 10^{-3}$. Some SM estimates of the mixing parameters x and y do not exclude mixing rates at the level reported here. Credible NP scenarios can also produce mixing rates of this level. Determining whether the $D^0 - \overline{D}^0$ mixing now being observed arises from SM long-distance effects, or from NP amplitudes, or some combination, requires more precise measurements of mixing in a variety of channels, more precise measurements of the SCS and DCS amplitudes which contribute to the SU(3) breaking used in the SM calculations, and better calculations.

REFERENCES

[1] A. Datta, D. Kumbhakar, *Z. Phys.* **C27**, 515 (1985).

[2] A.A. Petrov, *Phys. Rev.* **D56**, 1685 (1997).

[3] G. Burdman, I. Shipsey, *Annu. Rev. Nucl. Part. Sci.* **53**, 431 (2003).

[4] L. Wolfenstein, *Phys. Lett.* **B164**, 170 (1985).

[5] J.F. Donoghue, E. Golowich, B.R. Holstein, J. Trampetic, *Phys. Rev.* **D33**, 179 (1986).

[6] H. Georgi, *Phys. Lett.* **B297**, 353 (1992).

[7] T. Ohl, G. Ricciardi, E.H. Simmons, *Nucl. Phys.* **B403**, 605 (1993).

[8] A.A. Petrov, *Int. J. Mod. Phys.* **A21**, 5686 (2006).
[9] A.F. Falk, Y. Grossman, Z. Ligeti, Y. Nir, A.A. Petrov, *Phys. Rev.* **D69**, 114021 (2004).
[10] A.F. Falk, Y. Grossman, Z. Ligeti, A.A. Petrov, *Phys. Rev.* **D65**, 054034 (2002).
[11] E. Golowich, J. Hewett, S. Pakvasa, A.A. Petrov, *Phys. Rev.* **D76**, 095009 (2007).
[12] B. Aubert *et al., Phys. Rev. Lett.* **98**, 211802 (2007).
[13] M. Pivk, F.R. Le Diberder, *Nucl. Instrum. Methods* **A555**, 356 (2005).
[14] L.M. Zhang, *et al., Phys. Rev. Lett.* **96**, 151801 (2006).
[15] HFAG, `http://www.slac.stanford.edu/xorg/hfag/charm/`